Effects of Channel Wall Material on Performance and Plasma Characteristics of Hall Thrusters

IEPC-2005-015

Presented at the 29th International Electric Propulsion Conference, Princeton University, October 31 – November 4, 2005

Hirokazu Tahara*, Katsumi Imanaka+ and Seiro Yuge#
Graduate School of Engineering Science, Osaka University, Toyonaka, Osaka 560-8531, Japan

Abstract: The effects of channel wall material on Hall thruster performance and on plasma characteristics were investigated. A laboratory-model Hall thruster THT-III was operated with three channel wall materials of BN, BNSiN and BNAlN. Both the discharge current and the thrust were affected by the nature of the channel wall materials. The measured axial distributions of wall and plasma potentials, radial and axial electron temperatures, and electron number density near the channel walls showed that the wall material affected ionization region and ion wall loss in the channel, resulting from secondary electron emission, although ion acceleration region was determined by the axial distribution of radial magnetic field. The difference in discharge current between channel wall materials was considered to be caused by the difference in axial current density near the inner channel wall, depending on secondary electron emission.

I. Introduction

The closed-electron-drift Hall-effect thruster is a promising propulsion device in space. The performance has been improved in Russia since 1960s.[1] Because 1-2 kW class Hall thrusters can achieve a high performance of thrust 50-100 mN and thrust efficiency 40-50 % at specific impulses of 1000-2000 sec, they are expected to be used as main thrusters for near-earth missions in the United States and Europe.[2-4] Even in Japan, the high performance attracts attention of mission planners.[5-12]

It was early recognized that the nature of material used for walls of the acceleration channel had a significant effect on Hall thruster performance. The phenomenon is generally considered to be concerned with electrons emitted from the channel wall, i.e., secondary electron emission from the channel wall. The secondary emitted electrons have much lower temperature near the wall temperature than electrons in the bulk plasma have. As a result, a channel material with a high secondary electron emission coefficient cools the bulk plasma. However, the detail physics on the effect of channel wall material is still unclear.

In this study, the effects of channel wall material on thrust performance and on plasma characteristics in the vicinity of the channel wall are investigated using the laboratory-model Hall thruster THT-III. The operation is carried out for three channel wall materials: boron nitride (BN), boron nitride-silicon nitride mixture (BNSiN) and boron nitride-aluminum nitride mixture (BNAlN). The secondary electron emission coefficient of BN seems to be the highest in these materials. Discharge currents and thrusts are measured; specific impulses and thrust efficiencies are evaluated. Plasma parameters of wall and plasma potentials, radial and axial electron temperatures, and electron number density are measured with electrostatic single probes inside the acceleration channel. Radial profiles of discharge current density on the anode are also measured with radially-separated anodes. Relationships between the thrust performance and the plasma characteristics are discussed.

---

* Associate Professor, Department of Mechanical Science and Bioengineering, 1-3, Machikaneyama, E-mail: tahara@me.es.osaka-u.ac.jp, AIAA Member.
+ Graduate Student, Department of Mechanical Science and Bioengineering, 1-3, Machikaneyama,
# Graduate Student, Department of Mechanical Science and Bioengineering, 1-3, Machikaneyama, E-mail: yuge@arl.me.es.osaka-u.ac.jp.

II. Experimental Apparatus

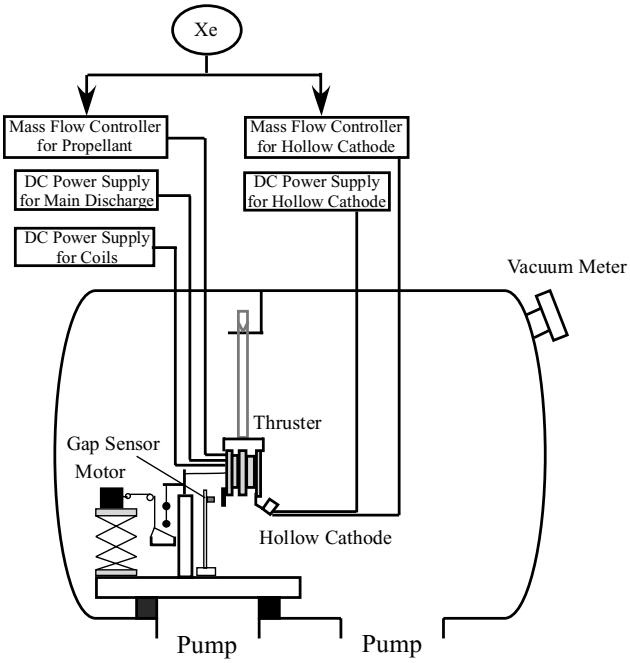

Figure 1. Experimental system for Hall thruster.

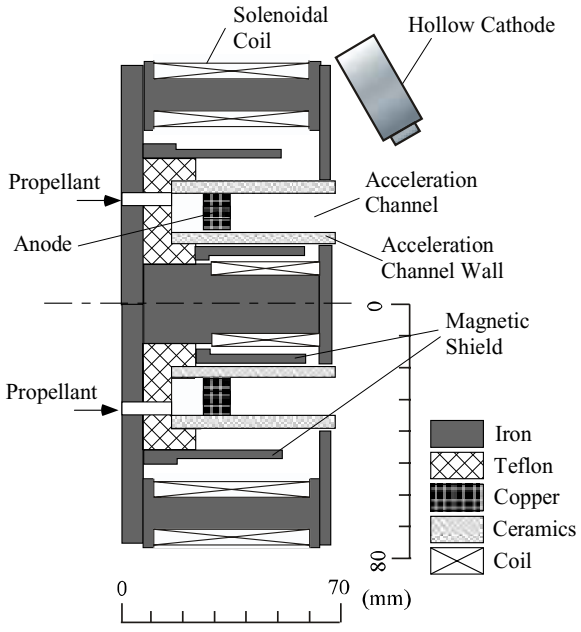

Figure 2. Cross-sectional view of Hall thruster THT-III.

The experimental facility, as shown in Fig.1, mainly consists of a water-cooled stainless steel vacuum tank 1.2 m in diameter x 2.25 m long, two compound turbo molecular pumps, several DC power supplies and a thrust measurement system.[6-8,12] The vacuum tank pressure is kept a range of 10^{-3}-10^{-4} Pa under operations.

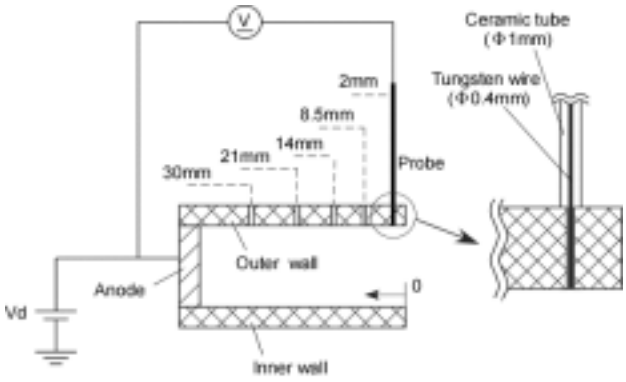

Figure 3. Probe measurement system of electric potential on outer wall in acceleration channel.

The THT-III Hall thruster, as shown in Fig.2, has an acceleration channel with an outer diameter of 70 mm and an inner diameter of 42 mm, i.e., with 14 mm in width, and with a channel length of 35 mm. The wall material of the acceleration channel is changed to commercial BN (BN: 99.5%), BNSiN (BN: 50%; Si_3N_4: 50%) and BNAlN (BN: 40%; AlN: 60%) ceramics. The secondary electron emission coefficient of BN seems to be the highest of three materials. The anode is made of copper. The hollow cathode (Iontech HCN-252) is used as the main cathode. After propellant gas is introduced from 4 lines into a plenum chamber behind the anode, it is uniformly injected from 16 ports azimuthally drilled on the anode into the acceleration channel. Xenon is used as the propellant. The thruster has a magnetic coil on the central axis and four coils outside the acceleration channel. Changing coil current varies the magnetic field strength in the acceleration channel. The magnetic field strength decreases as distance to the anode decreases, and it has a maximum near the channel exit and a minimum at the anode.

Thrusts are measured by a pendulum method. A Hall thruster is mounted on a thrust stand suspended with an aluminum bar, and the position of the thrust stand is detected by an eddy-current-type gap sensor (non-contacting micro-displacement meter). It has a high sensitivity and a good linearity. Thrust calibration is conducted with a weight and pulley arrangement which is able to apply a known force to the thrust stand under vacuum environment. With this design, friction force was small, and it resulted in no measurable hysteresis.

Plasma diagnostic measurement is carried out to understand phenomena near the acceleration channel wall and to infer features of the bulk plasma. Electric potential on the outer wall in the acceleration channel is measured as shown in Fig.3. Furthermore, plasma parameters of plasma potential, electron

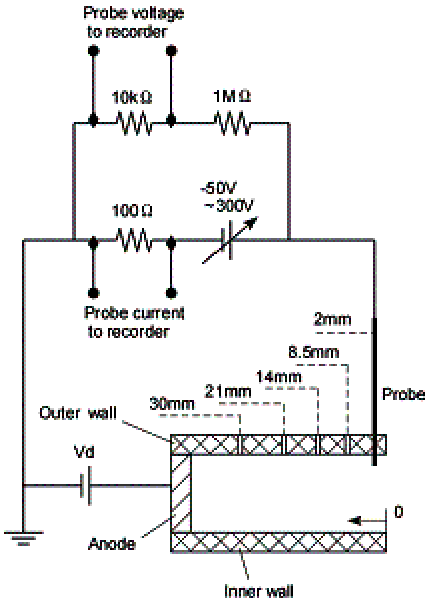

(a) Measurement system.

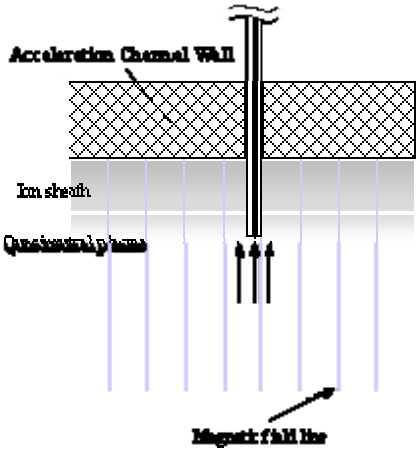

(b) Plasma parameters parallel to magnetic field.

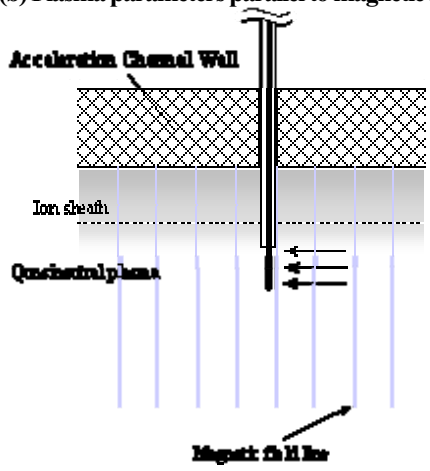

(c) Plasma parameters perpendicular to magnetic field.

Figure 4. Probe measurement system of plasma parameters near outer wall in acceleration channel.

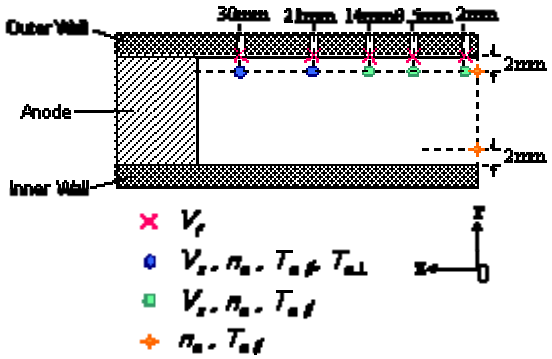

Figure 5. Measurement points and measured properties.

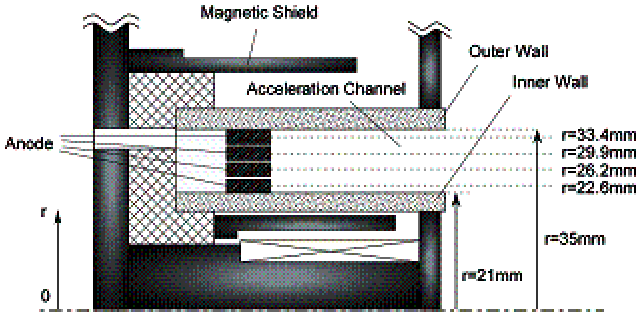

Figure 6. Measurement system of axial current density on anode with radially-separated anodes.

number density and electron temperatures perpendicular and parallel to magnetic field are measured with electrostatic single probes in the vicinity of the outer wall, as shown in Fig.4. The electron temperature perpendicular to magnetic field is measured near the anode where the radial magnetic field is relatively weak. Plasma parameters are also measured in the vicinity of the inner wall at the channel exit. The measurement points inside the acceleration channel are summarized in Fig.5. In order to understand axial current conduction, radial profiles of discharge current density on the anode are also measured with radially-separated anodes shown in Fig.6.

III. Results and Discussion

A. Performance Characteristics Dependent on Channel Material Species

Figure 7 shows the performance characteristics dependent on maximum magnetic field strength with channel wall materials of BN, BNSiN and BNAlN at a discharge voltage of 200 V with a mass flow rate of 2 mg/s. The discharge current for BNAlN is the highest at all magnetic field strengths, and those for BN and BNSiN are almost equal. The thrust and the specific impulse are

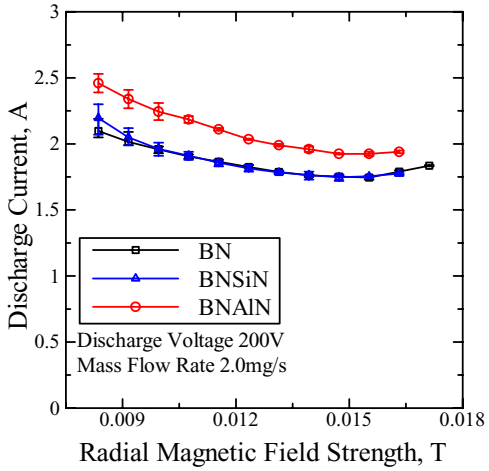

(a) Discharge current.

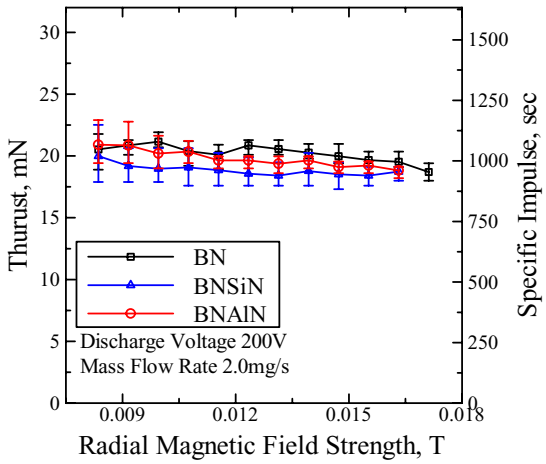

(b) Thrust and specific impulse.

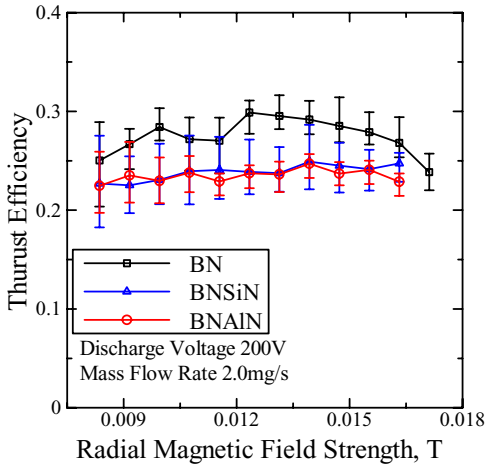

(c) Thrust efficiency.

Figure 7. Performance characteristics dependent on maximum magnetic field strength with channel wall materials of BN, BNSiN and BNAlN at 200 V and 2 mg/s.

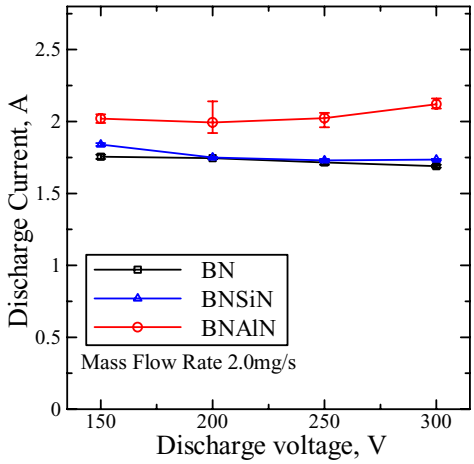

(a) Discharge current.

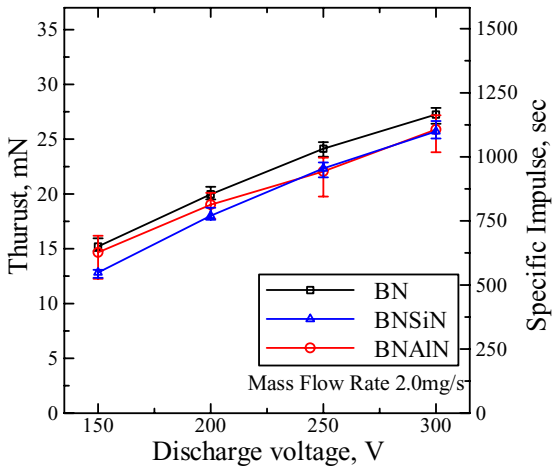

(b) Thrust and specific impulse.

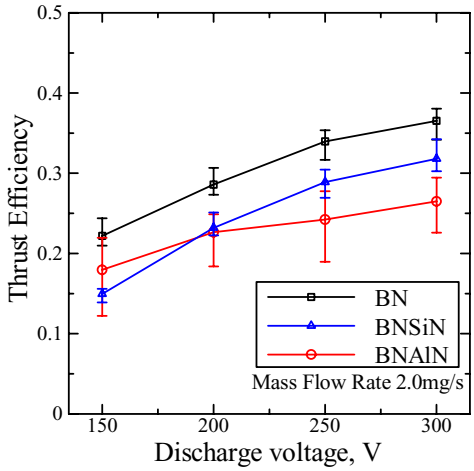

(c) Thrust efficiency.

Figure 8. Performance characteristics dependent on discharge voltage with three wall materials for optimum magnetic field strengths at 2 mg/s.

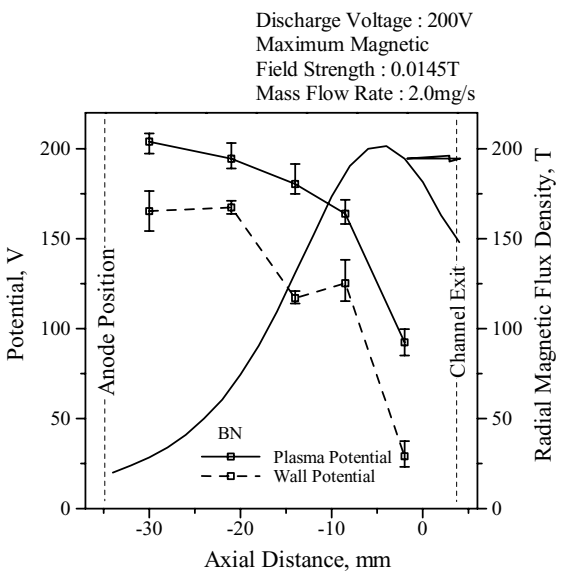

(a) BN with magnetic field shape.

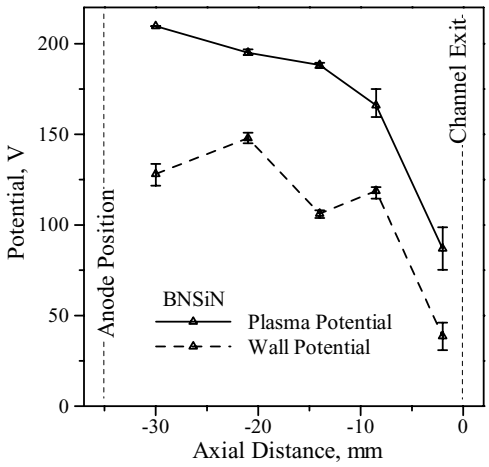

(b) BNSiN.

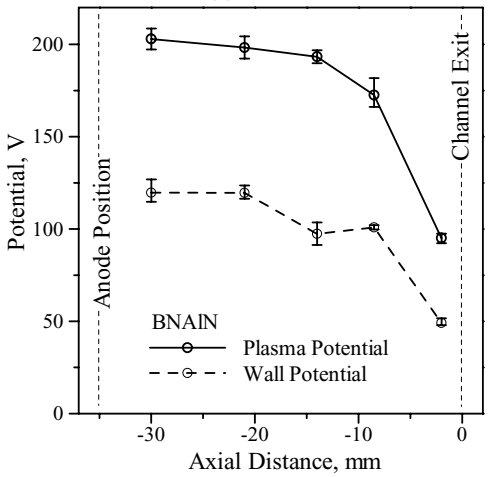

(c) BNAlN.

Figure 9. Axial distributions of potentials on and near outer wall with BN, BNSiN and BNAlN at 200 V and 2 mg/s.

the highest with BN, and those are the lowest with BNSiN.

Figure 8 shows the performance characteristics dependent on discharge voltage with three channel wall materials for the optimum magnetic field strengths at 2 mg/s. The discharge current for BNAlN is the highest at all discharge voltages, and those for BN and BNSiN are almost equal. The thrust and the specific impulse are the highest with BN at all discharge voltages and the lowest with BNSiN. For BNAlN, they are almost equal to those with BN at a low discharge voltage of 150 V, but they are approaching those with BNSiN as increasing discharge voltage.

As a result, the thrust efficiency is the highest with BN at all magnetic field strengths and all discharge voltages, as shown in Figs.7(c) and 8(c). Both the discharge and the thrust are found to be intensively affected by nature of channel wall materials.

B. Inner Plasma Characteristics Dependent on Channel Material Species

Figure 9 shows the axial distributions of wall potential on the outer wall of the acceleration channel and plasma potential near the outer wall with channel wall materials of BN, BNSiN and BNAlN at a discharge voltage of 200 V and a mass flow rate of 2 mg/s. Both the wall potential and the plasma potential intensively decrease downstream from -8.5 mm, i.e., near an axial position of the maximum radial magnetic field strength, as shown in Fig.9(a), regardless of wall material species. The difference between wall potential and plasma potential is the smallest with BN but the largest with BNAlN. Because the difference between the potentials is concerned with secondary electron emission effect of dielectric wall, the secondary electron emission coefficient of BN is predicted to be the highest of three materials and that of BNAlN the lowest.

Figure 10 shows the axial distributions of plasma properties near the outer wall with three channel wall materials at 200 V and 2 mg/s. The electron number densities for BN and BNAlN, as shown Fig.10(a), have peaks at -14 mm, and the peak value for BN is higher than that for BNAlN. On the other hand, BNSiN material has a lower peak at -8.5 mm. The radial electron temperature for BN, as shown in Fig.10(b), has a high value around 13 eV from -2 to -8.5 mm and rapidly decreases upstream from -8.5 mm. However, because the radial electron temperatures for BNSiN and BNAlN decrease upstream from the channel exit, i.e., from -2 to -8.5 mm, peaks of radial electron temperature for the both gases are expected to exist near the channel exit or in the downstream region. The axial electron temperature, as shown in Fig.10(c), is the smallest with BN in the upstream region.

Figure 11 shows the radial distributions of plasma properties at the channel exit, at an axial position of 0 mm, for three channel wall materials with 200 V and 2 mg/s. The electron number density near the inner wall of the acceleration channel is higher than that on the outer wall although the profile for BN is almost radially flat. Particularly, for BNAlN the electron density near the inner wall is much higher. Near both the inner and outer walls, the electron density for BNAlN is the highest of three wall

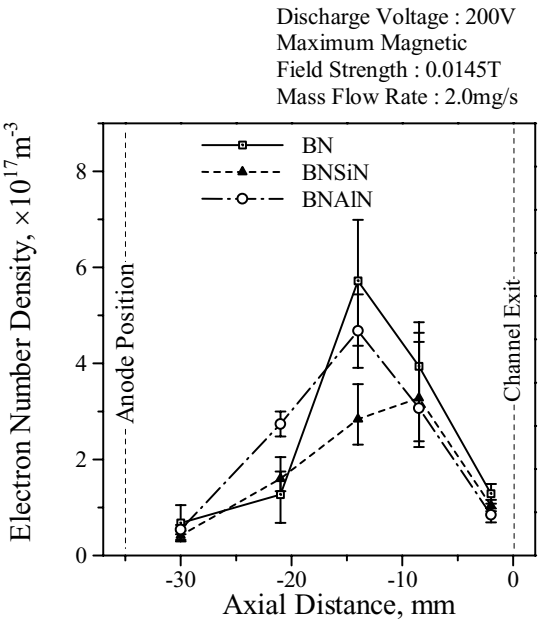

(a) Electron number density.

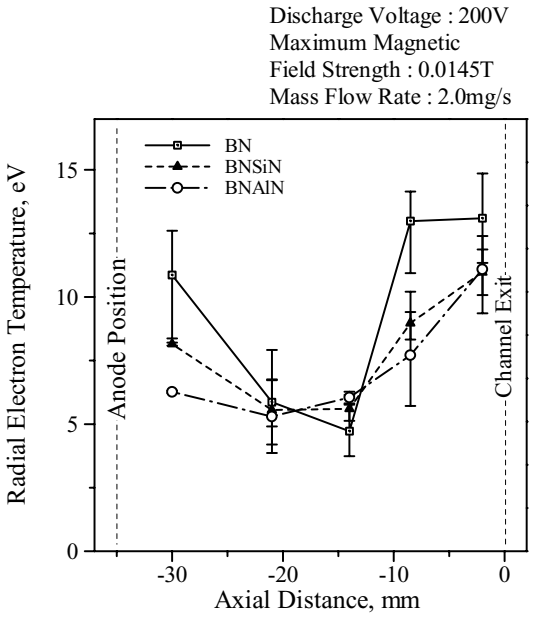

(b) Electron temperature parallel to radial magnetic field.

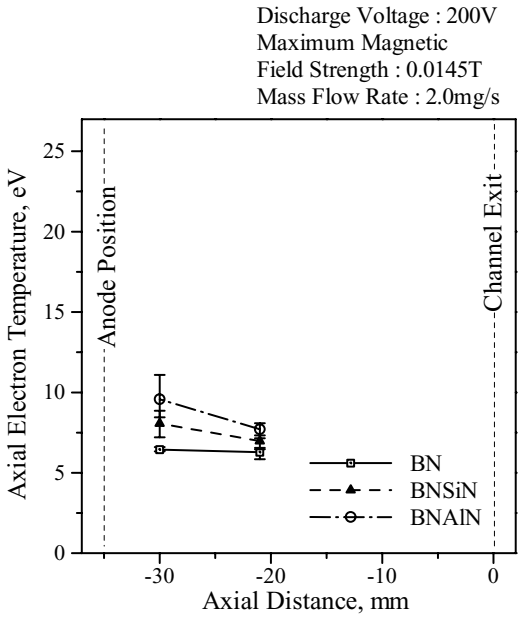

(c) Electron temperature perpendicular to radial magnetic field.

Figure 10. Axial distributions of electron number density and electron temperatures parallel and perpendicular to radial magnetic field near outer wall with channel wall materials of BN, BNSiN and BNAlN at discharge voltage of 200 V and mass flow rate of 2 mg/s.

materials but for BN the lowest. As shown in Fig.11(b), the radial electron temperature almost has the same characteristic. Accordingly, because the magnetic field strength near the inner wall is larger than that near the outer wall, intensive ionization is expected to occur near the inner wall of BNAlN with the lowest secondary electron emission coefficient.

In plasma production and acceleration processes with the BN channel wall, the following feature is expected. When electrons emitted from the hollow cathode, as shown in Fig.12, enter the acceleration channel and ionize neutral particles, the high-temperature plasma electrons are slightly cooled by low-temperature electrons emitted from the BN channel wall due to intensive secondary electron emission effect. As a result, the peak of electron temperature is located near the axial position of the maximum of magnetic

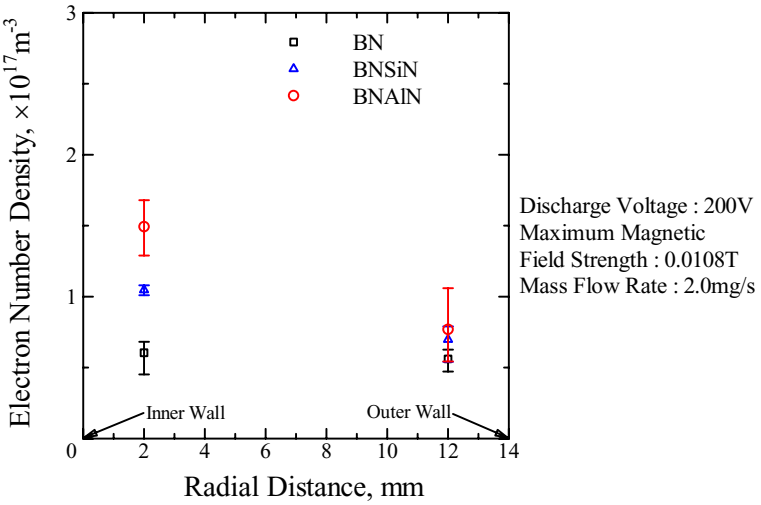

(a) Electron number density.

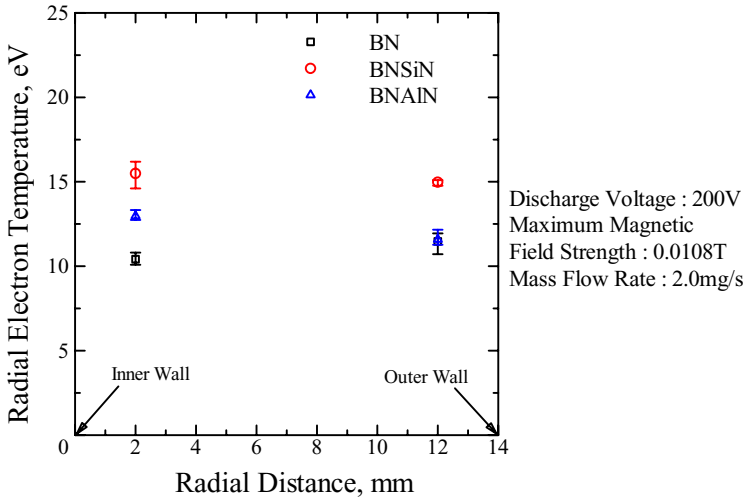

(b) Electron temperature parallel to radial magnetic field.

Figure 11. Radial distributions of electron number density and electron temperature parallel to radial magnetic field at channel exit, at axial position of 0 mm, for channel wall materials of BN, BNSiN and BNAlN at discharge voltage of 200 V and mass flow rate of 2 mg/s.

field strength, and then an intensive ionization occurs; just downstream from that, the produced ions are efficiently accelerated with the deep potential drop shown in Fig.9. On the other hand, in the cases with the BNSiN and BNAlN walls as shown in Fig.10(b), the plasma electrons are not cooled in the acceleration channel, specially near the channel exit, because of the lower secondary electron emission coefficients. As a result, because the peak of electron temperature is located near the channel exit, i.e., at a point downstream from the axial position of the maximum of magnetic field strength, as expected from data near the outer wall in Fig.11(b), the produced ions are not accelerated efficiently.

In other words, it is considered that the channel wall material affects an axial position of ionization region. On the other hand, an axial position of ion acceleration region is generally determined by the radial magnetic field shape. In the case of the BN channel wall, because of the highest secondary electron emission coefficient, the ionization region is near the ion acceleration region, and the produced ions would be efficiently accelerated.

Furthermore, ion loss process is predicted from the potential distributions shown in Fig.9 as follows. Because the BNAlN wall has the largest difference between wall and plasma potentials, the produced ions are radially attracted to the channel wall by a large radial electric field in a presheath and a sheath; i.e., large ion losses on the channel wall are suspected to take place. On the other hand, for BN ion wall losses are relatively small because of the smallest potential difference.

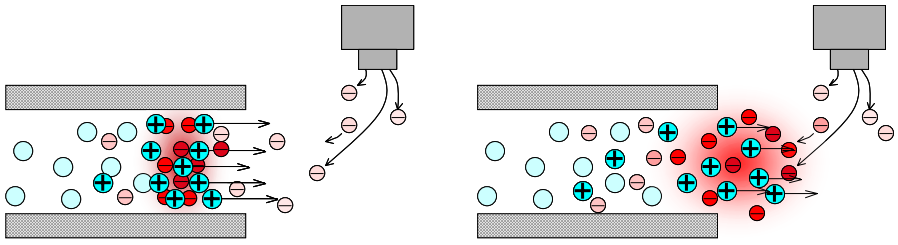

(a) BN. **(b) BNSiN and BNAlN.**

Figure 12. Plasma production and ion acceleration processes.

These diagnostic results and predictions agree with the thrust characteristics measured as shown in Figs.7(b) and 8(b).

C. Current Density Characteristics on Anode Dependent on Channel Material Species

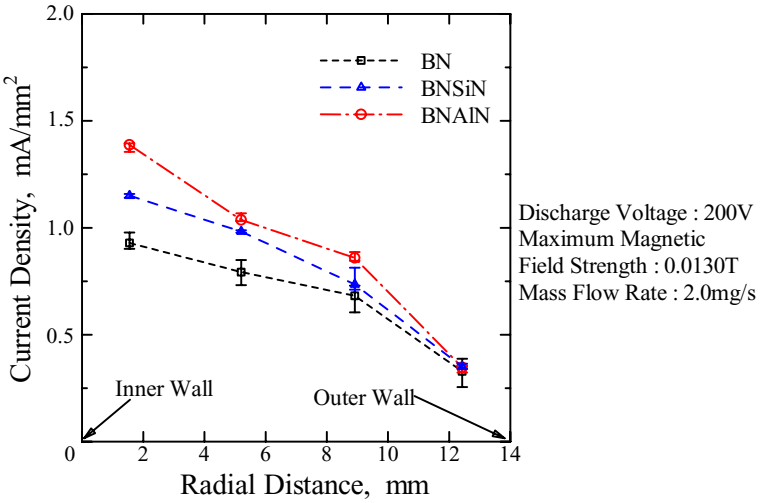

Figure. 13 Radial profiles of discharge current density on anode with channel wall materials of BN, BNSiN and BNAlN at discharge voltage of 200 V and mass flow rate of 2 mg/s.

Figure 13 shows the radial profiles of discharge current density on the anode with channel wall materials of BN, BNSiN and BNAlN at a discharge voltage of 200 V and a mass flow rate of 2 mg/s. The current density increases radially-inward regardless of channel material species. The current density is the lowest with BN near the inner wall and the highest with BNAlN although they are almost equal near the outer wall.

This is expected because both the electron temperature and the electron number density for BN, as shown in Fig.11, are the lowest near the inner wall due to intensive secondary electron emission, resulting in poor axial electron conduction. On the other hand, those for BNAlN are kept high near the inner wall. As shown in Fig.14, the difference in current conduction between wall materials is expected to mainly occur near the inner channel wall, depending on secondary electron emission.

These results and predictions agree with the current characteristics measured as shown in Figs.7(a) and 8(a).

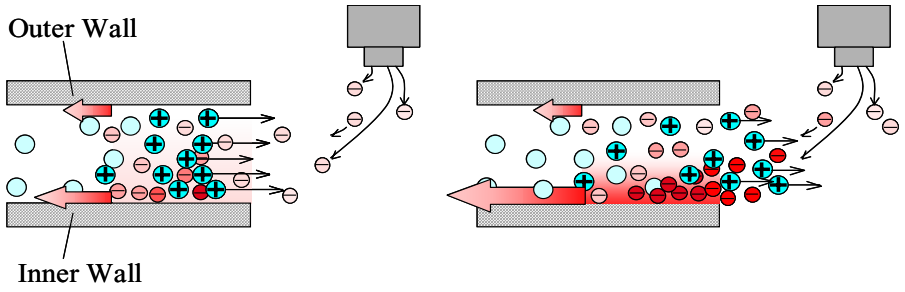

(a) BN. **(b) BNAlN.**

Figure 14. Near-wall current conduction process.

IV. Conclusions

The effects of channel wall material on thrust performance and plasma characteristics were investigated using the laboratory-model Hall thruster THT-III. Three channel wall materials of BN, BNSiN and BNAlN were used. The following results were mainly obtained.

1) The thrust efficiency was the highest with BN at all magnetic field strengths and all discharge voltages. Both the discharge and the thrust were considered to be intensively affected by nature of channel wall materials.

2) The measured plasma characteristics showed that channel wall material affected an axial position of ionization region. On the other hand, an axial position of ion acceleration region was expected to be determined by the radial magnetic field shape. In the case of the BN channel wall, because of the highest secondary electron emission coefficient, the ionization region was near the acceleration region,

and then the produced ions would be efficiently accelerated. Furthermore, because the BNAlN wall had the largest difference between wall and plasma potentials, the produced ions were suspected to be radially attracted to the channel wall by a large radial electric field in a presheath and a sheath; i.e., large ion losses on the channel wall were suspected to occur. On the other hand, for BN ion wall losses were relatively small because of the smallest potential difference.

3) The current density on the anode increased radially-inward regardless of channel material species. The current density was the lowest with BN near the inner wall and the highest with BNAlN although they were almost equal near the outer wall. This was expected because both the electron temperature and the electron number density for BN were the lowest near the inner wall due to intensive secondary electron emission, resulting in poor axial electron conduction. On the other hand, those for BNAlN were kept high near the inner wall. The difference in current conduction between wall materials was mainly expected to take place near the inner channel wall, depending on secondary electron emission.

It is necessary to select preferable relationships between channel wall material properties and magnetic field structure for development of high-performance Hall thruster.

References

[1] Kim, V.," Main Physical Features and Processes Determining the Performance of Stationary Plasma Thrusters," *Journal of Propulsion and Power*, Vol.14, pp.736-743, 1998.

[2] Dunning, J.W., Benson, S., and Oleson, S.," NASA's Electric Propulsion Program," *27th International Electric Propulsion Conference, Pasadena*, Paper No.IEPC 01-002, 2001.

[3] Cadiou, A., Gelas, C., Darnon, F., Jolivet, L., and Pillet, N.," An Overview of the CNES Electric Propulsion Program," *28th International Electric Propulsion Conference, Toulouse*, Paper No.IEPC 03-169, 2003.

[4] Milligan, D., Gestal, D., Camini, O., Estublier, D., and Koppel, C.," SMART-1 Electric Propulsion Operations," AIAA Paper No.2004-3436, 2004.

[5] Kuninaka, H.," Activities on Electric Propulsion in Japan -Space Flight from Basic Research-," *38th AIAA/ASME/SAE/ASEE Joint Propulsion Conference and Exhibit, Indianapolis*, AIAA Paper No.2002-3563, 2002.

[6] Tahara, H., Goto, D., Yasui, T., and Yoshikawa, T.," Thrust Performance and Plasma Characteristics of Low Power Hall Thrusters," *27th International Electric Propulsion Conference, Pasadena*, Paper No.IEPC 01-042, 2001.

[7] Tahara, H., Goto, D., Yasui, T., and Yoshikawa, T.," Thrust Performance and Plasma Features of Low-Power Hall-Effect Thrusters," *Vacuum*, Vol.65, pp.367-374, 2002.

[8] Kitano, T., Fujioka, T., Shirasaki, A., Goto, D., Tahara, H., Yasui, T., Yoshikawa, T., Fuchigami, K., Iinoya, F., and Ueno, F.," Research and Development of Low Power Hall Thrusters," *23rd International Symposium on Space Technology and Science, Matsue*, Paper No.ISTS 2002-b-18, 2002.

[9] Shirasaki, A., Tahara, H., and Martinez-Sanchez, M.," One-Dimensional Flowfield Calculation of Hall Thrusters," *23rd International Symposium on Space Technology and Science, Matsue*, Paper No.ISTS 2002-b-33p, 2002.

[10] Tahara, H., Fujioka, F., Shirasaki, A., and Yoshikawa, T.," Simple One-Dimensional Calculation of Hall Thruster Flowfields," *28th International Electric Propulsion Conference, Toulouse*, Paper No.IEPC 03-016, 2003.

[11] Tahara, H., Yuge, S., Shirasaki, A., and Martinez-Sanchez, M.," Performance Prediction of Hall Thrusters Using One-Dimensional Flowfield Calculation," *24th International Symposium on Space Technology and Science, Miyazaki*, Paper No.ISTS 2004-b-53p, 2004.

[12] Tahara, H., Shirasaki, A., Yuge, S., and Yoshikawa, T.," Optimization of Magnetic Field and Acceleration Channel for Low Power Hall Thrusters," *Proceedings of the 24th International Symposium on Space Technology and Science*, pp.264-273, 2004.